ELSEVIER

Journal of Photochemistry and Photobiology A: Chemistry 142 (2001) 177–185

Journal of Photochemistry and Photobiology A:Chemistry

www.elsevier.com/locate/jphotochem

Resonance Raman study of ring deuterated 4-dimethylaminobenzonitrile (DMABN-d_4): the ground, ICT and triplet states

C. Ma [a,*], W.M. Kwok [a], P. Matousek [b], A.W. Parker [b], D. Phillips [a], W.T. Toner [c], M. Towrie [b]

[a] *Department of Chemistry, Imperial College, Exhibition Road, London SW7 2AY, UK*
[b] *Central Laser Facility, CLRC Rutherford Appleton Laboratory, Didcot, Oxfordshire OX11 0QX, UK*
[c] *Department of Physics, Clarendon Laboratory, Parks Road, Oxford OX1 3PU, UK*

Abstract

Picosecond and nanosecond time-resolved resonance Raman spectra of the intramolecular charge transfer (ICT) and triplet state of DMABN-d_4 have been obtained over the frequency range from 650 to 2250 cm^{-1}. The spectra and the isotopic shifts observed on going from normal DMABN to the ring deuterated analogue are interpreted with the aid of DFT vibrational analysis of ground state spectra and comparisons made with closely related compounds. The data confirm our previous results but the isotopic shifts induced by the ring deuteration provide additional evidence clarifying the planar structure of the triplet state and indicating full localisation of negative charge on the cyano group.

Keywords: 4-Dimethylaminobenzonitrile (DMABN); Intramolecular charge transfer reaction; TICT; Triplet state

1. Introduction

4-Dimethylaminobenzonitrile (DMABN) is an archetypal intramolecular electron donor–acceptor molecule that has attracted the interest of both experimentalists and theoreticians during the last 40 years [1]. The solvent dependent dual fluorescence has been interpreted in terms of an intramolecular charge transfer (ICT) reaction from a locally excited (LE) to an ICT state occurring only in polar solvents. A conjugated planar structure has been predicted for the LE state [2–6]. Several models, twisted ICT (TICT) [7], wagged ICT (WICT) [8], planar ICT (PICT) [9], and rehybridisation ICT (RICT) [10], were proposed to describe the geometry of the ICT state. The TICT model was supported very recently by picosecond Kerr gate time-resolved resonance Raman measurements (ps-K-TR^3) [2,11,12] and time-resolved infrared (TRIR) studies [3,13,14]. It is also supported by most theoretical work including recent calculations with and without the effects of the solvent by Mennucci et al. [15] and Dreyer and Kummrow [4], respectively.

The triplet state of DMABN has also been studied extensively both experimentally [13,16–21] and theoretically [5,6,22–24]. Intersystem crossing (ISC) has been shown to be the principal non-radiative deactivation channel for the singlet states, irrespective of solvent polarity [17–19]. Most work suggests the lowest triplet state ($^3T_1$) of DMABN is a planar $\pi\pi^*$ state and only this triplet state is active in the $^3T_1 \rightarrow S_0$ intersystem crossing and phosphorescence processes [18–20,22–24]. However, this view is challenged by TRIR studies performed by Hashimoto and Hamaguchi that identify a ^{3}TICT state in polar solvent [13]. This leads to a controversy concerning both the triplet geometry (planar or TICT?) and the ISC mechanism.

In our previous work, the ICT [2,11,12] and triplet [25] states of DMABN have been studied in various solvents using time-resolved techniques, such as ps-K-TR^3, ns-TR^3 and transient absorption. Comparison of transient Raman spectra of normal DMABN with corresponding spectra of the amino nitrogen isotopic compound (DMABN-^{15}N, identified as ^{15}N below) and the compound with deuterated methyl groups (DMABN-d_6, identified as d_6 below) was used to identify bands associated with vibrations of dimethylaniline subgroup. The analysis was based on frequencies of the cyano stretching (C≡N) and amino nitrogen-ring stretching (ν(ph-N)) vibrations and their relative shifts from corresponding ground state bands. Structures corresponding to the electronic twisted decoupled and planar or near-planar diradical have been suggested for the ICT and triplet state, respectively. In addition, the similarity of the frequencies of the amino group modes in the ICT state and the protonated dimethylaniline (DMA-H$^+$) molecule has been taken to indicate some pyramidal character for the structure of the ICT state [12].

* Corresponding author.
E-mail address: c.ma@ic.ac.uk (C. Ma).

1010-6030/01/$ – see front matter
PII: S1010-6030(01)00512-3

We have also obtained time-resolved Raman spectra of the ICT and triplet states of phenyl ring deuterated DMABN, DMABN-d_4 (identified as d_4 below), with the aim of identifying the DMABN bands due to ring CH bending vibrations. However, due to extensive vibrational coupling, especially between ring CC stretching and CH bending modes, band shifts observed in the d_4 spectra are too complex to allow direct assignments. Very recently, we made density function theoretical (DFT) ab initio calculations (B3YLP/6-31G* basis set) to interpret the ground state normal Raman spectrum and isotopic shifts on going from d_0 to d_4. Good agreement between the computed and experimental spectra was obtained [26]. This makes it possible to assign the transient bands observed in spectra of the ICT and triplet states of d_4. In this paper, we report a resonance Raman study of the ground, ICT and triplet states of d_4 that complements our previous work. The properties of these states are discussed and compared with closely related compounds.

2. Experimental

The ps-K-TR^3 spectrum of the ICT state of d_4 was obtained using the same arrangement as described in [2,11,12]. The pump and probe wavelengths of 267 and 330 nm were generated by frequency tripling the fundamental output of the regenerative amplifier and an optical parametric amplifier (OPA) respectively as described elsewhere [27,28]. Details of acquisition methods and the Kerr gate are given in [29]. Here we used an improved system based on a benzene Kerr gate with throughput of 20% (excluding polariser losses). A solution filter of *trans*-stilbene was used to block the Rayleigh and scattered pump light. The filter cuts off bands below 650 cm^{-1} and attenuates intensities for frequencies below 900 cm^{-1}. Each spectrum shown is the sum of three individual background-subtracted spectra with accumulation times typically of 2000 s.

Since both the ground and ICT state of DMABN absorb in the 330 nm region, the ground state resonance Raman spectrum and transient resonance Raman (TR^2) spectra of d_4 were obtained at this wavelength by the single-colour pump-probe method. The nanosecond instrument arrangement and experimental conditions are the same as those given in [12]. The TR^2 spectra presented here resulted from subtraction of normalised low laser power (~0.1 mJ per pulse) spectra and solvent spectra from high power (~0.5 mJ per pulse) spectra. The ground state resonance Raman spectra were obtained by subtracting normalised high laser power spectra and solvent spectra from the low power spectra. The total accumulation times for the high and low power spectra were about 1 and 2 hours, respectively.

The ns-TR^3 spectra were obtained using the system described in [25] with 90° signal collecting configuration and a liquid nitrogen cooled CCD detector. The laser wavelengths were 308 (excimer laser, pump) and 532 nm (the second harmonic output of a Nd:YAG laser, probe) pulses at a repetition rate of 10 Hz. The sample solution was circulated through a quartz sample tube (3 mm diameter). Argon was bubbled through the reservoir to remove oxygen during the experiment. Nitrogen bubbling gave similar spectra but oxygen bubbling quenched the Raman signal. Spectra presented here were accumulated totally over ~100 min. with pump only and probe only spectra being subtracted.

Acetonitrile (fresh solution) Raman bands were used to calibrate all the spectra with an estimated accuracy in absolute frequency of $\pm 10\,cm^{-1}$ for the ps-K-TR^3 and $\pm 5\,cm^{-1}$ for the ns-TR^3 and TR^2 spectra, respectively. The spectra were not corrected for variations in throughput and detector efficiency.

Spectroscopic grade solvents were used as received. DMABN-d_4 was synthesised according to [8,30,31], and purity was confirmed by NMR and mass spectroscopic analysis. Sample concentrations were 1×10^{-3} to 5×10^{-3} mol dm^{-3} for all the experiments. The UV absorption measurements before and after sample use revealed no degradation.

3. Results and discussion

The Raman spectra presented here cover the 650–2250 cm^{-1} region. Fig. 1a shows the ground state resonance Raman spectrum of d_4 in methanol recorded at 330 nm excitation wavelength. Transient Raman spectra of the ICT state of d_4 in the same solvent are displayed in Fig. 2, which includes both the TR^2 spectrum (a) and the ps-K-TR^3 spectrum at 50 ps delay time (b). The ns-TR^3 spectrum of d_4 obtained in hexane solvent at 50 ns delay time is given in Fig. 3a. This spectrum is assigned to the triplet state as bubbling the solution with oxygen quenched the signal and the probe wavelength falls into the known absorption band of the triplet state. A similar ns-TR^3 spectrum was obtained in methanol solvent but with poorer S/N ratio due to the red fluorescence. This indicates that formation of the triplet state is independent of solvent polarity, which is consistent with previous results of transient absorption studies [16,19,20]. For comparison and to justify the spectral assignments, the corresponding spectra of DMABN (identified as d_0 below) obtained under the same experimental conditions [12,25] are displayed together with the d_4 spectra in all the figures.

Table 1 lists frequencies and relative intensities of the resonance Raman bands observed for d_4 as calculated from unconstrained fitting of the bands to Lorentzian band shape. Band assignments and vibrational data of the closely related compounds, ring deuterated dimethylaniline [32–34] (DMA-d_5, identified as d_5 below), are also included in the Table.

3.1. Ground state resonance Raman spectrum

Our DFT calculation and Raman spectroscopy study [26] show that frequency shifts are not restricted to the ring CH

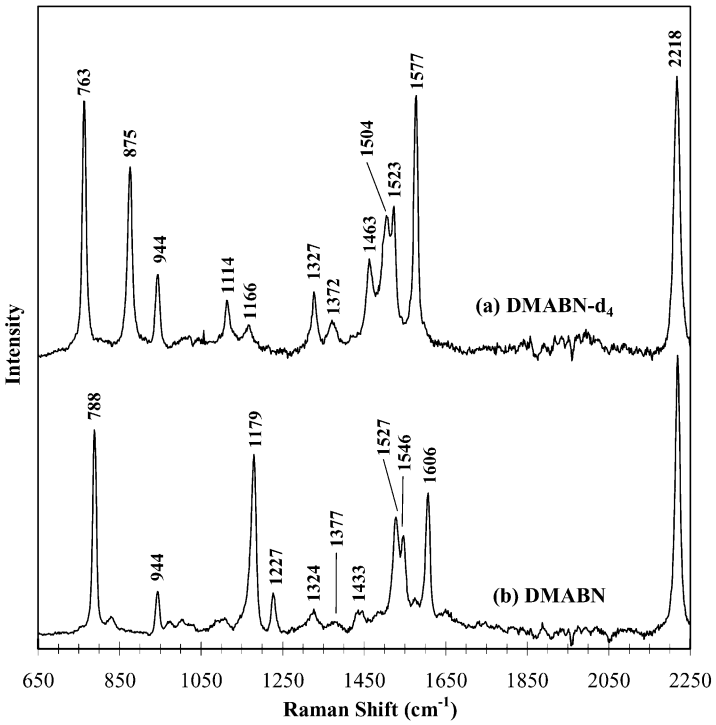

Fig. 1. Resonance Raman spectra of ground state of DMABN-d_4 (a) and DMABN (b) in methanol obtained at 330 nm excitation.

modes since there are also complex changes in the vibrational coupling between these and other modes within the deuterated molecule that affect both frequencies and intensities. The assignments of d_4 ground state bands given in Table 1 are based on the DFT results. Several points relating to the typical band shifts and variations of vibrational features on going from d_0 to d_4 are worthy of discussion since they form the basis of our interpretation of the excited state spectra of d_4.

Bands dominated by the ring CC stretching vibrations were found to downshift by ~20–30 cm^{-1} upon ring deuteration. Three such modes were observed as seen in Fig. 1 the ring CC stretching Wilson 8a (1577 cm^{-1} in d_4 and 1606 cm^{-1} in d_0) and 8b (1523 cm^{-1} in d_4 and 1546 cm^{-1} in d_0) and the ring breathing Wilson 1 (763 cm^{-1} in d_4 and 788 cm^{-1} in d_0). The ring CH in plane bending mode (Wilson 9a) downshifts characteristically by ~300 cm^{-1} from 1179 cm^{-1} in d_0 to 875 cm^{-1} in d_4.

Bands showing significant changes brought about by changes in the vibrational coupling upon ring deuteration are those mainly associated with the ring-substitutent stretching vibrations, i.e. the ν(ph-CN), ν(ph-N), and the ring CC stretching described by Wilson 19b and 19a. These are found in d_0 at 1227, 1377, 1433 and 1527 cm^{-1} (Fig. 1b). These bands show strong mixing. For example, the 1527 cm^{-1} 19a band of d_0 has substantial contributions from ν(ph-N) and the ring CH in plane bending vibration (the Wilson 18a). The d_0 bands at 1527, 1433 and 1377 cm^{-1} correspond to those observed at 1417, 1372 and 1327 cm^{-1} in d_4, the latter two are seen in Fig. 1a. Taking also the 1527 cm^{-1} (19a dominated) band of d_0 for example, the variation in vibrational mixing upon ring deuteration is indicated by a smaller contribution of the CH bending motion than there is in its d_0 equivalent [26]. This is probably related to the unusually large down shift ($\Delta\nu \approx 100\ cm^{-1}$) on going from d_0 to d_4. However, in contrast to this and confirmed by DFT calculations [26], the 1227 cm^{-1} band of d_0 (Fig. 1b) disappears upon ring deuteration. In its place, a band at 1114 cm^{-1} (Fig. 1a) is observed in d_4 that results from strong mixing of the ν(ph-CN), ν(ph-N) vibrations coupled with the 19a and several other motions. The band can be represented approximately by the Wilson 7a [35] stretch. Furthermore, as illustrated below, this replacement of one band at ~1220 cm^{-1} in d_0 by another at ~1100 cm^{-1} in d_4 also occurs in the corresponding excited state spectra.

In Fig. 1, bands of d_4 observed at 1504, 1463 and 1166 cm^{-1} are assigned to normal modes associated with the methyl group using our DFT results [26]. The absence of these modes in the spectrum of d_0 (Fig. 1b) is probably due to a different resonance enhancement for these modes when using 330 nm Raman excitation wavelength and caused by a redistribution of the potential energy related to these modes upon ring deuteration [33]. The 944 cm^{-1} band observed in spectra of both d_0 and d_4 (Fig. 1) is assigned to the symmetric amino nitrogen-methyl stretch ($\nu^s(NC_2)$) and as expected this mode is insensitive to ring deuteration [26,36].

From Table 1, one is readily able to identify similarities between the vibrational frequencies of d_4 and DMA-d_5.

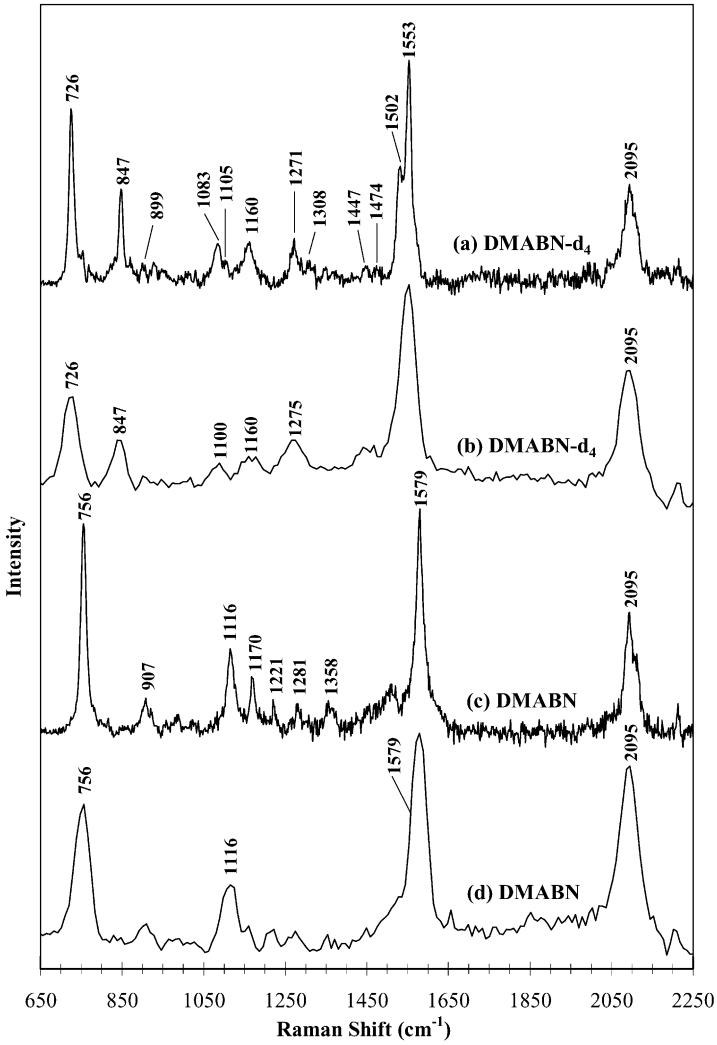

Fig. 2. Resonance Raman spectra of the ICT states. Transient resonance Raman spectra of DMABN-d_4 (a) and DMABN (c) obtained at 330 nm excitation in methanol. The ps-Kerr-gated time-resolved resonance Raman spectra of DMABN-d_4 (b) and DMABN (d) in methanol obtained at 267 nm pump, 330 nm probe wavelengths at 50 ps delay time.

However, it is interesting to note the fairly large difference in frequency for the ν(ph-N) vibration, which was found at 1327 and 1298 cm^{-1} for d_4 and d_5, respectively. This indicates a stronger nπ conjugation between the nitrogen lone pair and aromatic π-ring system in d_4 brought about by the presence of the cyano, an electron withdrawing group at the *para* position to the amino group. This leads to the ph-N bond in d_4 having more double bond character than in d_5. This is in accordance with the more nearly-planar geometry of DMABN in comparison to DMA as reported from X-ray diffraction and microwave studies which conclude that the wagging angle between the amino and ring group is $\sim 11^\circ$ for DMABN [37,38] and 27° for DMA [39].

The spectra of the ICT and triplet states of d_4 (Figs. 2a and b and 3a) are interpreted using the isotopic effect described above and by comparison with corresponding forms of d_5, the d_5-H^+ for the ICT state and radical cation of d_5 for the triplet state, respectively. The Raman bands observed in the excited states of d_4 are assigned in term of totally symmetric modes.

3.2. The ICT state

The 330 nm probe wavelength used in the ps-K-TR^3 and TR^2 experiments lies in the strong absorption band of the DMABN ICT state identified by Okada et al. [40]. From Fig. 2, it is clear that data from the TR^2 spectra offer superior spectral resolution to the ps-K-TR^3 spectra at the expense of the observation of short time scale kinetics. For example, the broad features of d_4 at 1275, 1100 cm^{-1} observed in the ps-K-TR^3 spectrum (Fig. 2b) are each resolved into two bands, 1308/1271, and 1105/1083 cm^{-1} in the TR^2 spectrum (Fig. 2a). Complete subtraction of the ground state Raman signal is evident from obvious differences between the spectra in Fig. 2a and c and those in Fig. 1a and b. resemblance of the TR^2 (Fig. 2a and c) to ps-K-TR^3 spectra

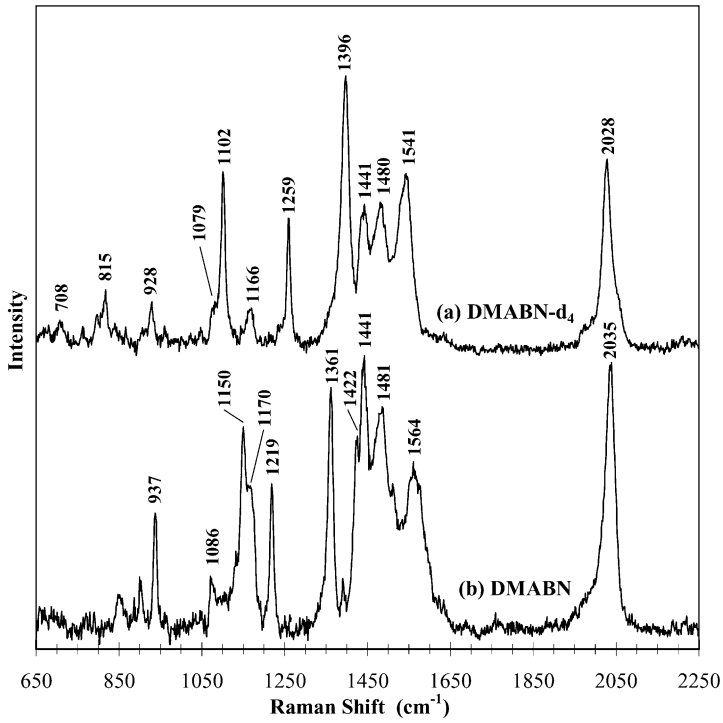

Fig. 3. Nanosecond time-resolved resonance Raman spectra of the lowest triplet state of DMABN-d_4 (a) and DMABN (b) in hexane obtained at 308 nm pump and 532 nm probe wavelengths at 50 ns delay time.

(Fig. 2b and d) means that they originate from the same excited state, the ICT state, as identified from the 2095 cm^{-1} C≡N frequency. This band serves as a marker to identify the state being probed [2,3,11–13,41,42]. However, the band at 1502 cm^{-1} is only observed in the TR^2 spectrum (Fig. 2a). It appears as the shoulder of the strong 1553 cm^{-1} band, as seen in Fig. 2a. The intensity of this band relative to the others in Fig. 2a shows both probe wavelength and solvent dependence. This indicates that rather than the unresolved band in the ps-K-TR^3 spectra (Fig. 2b), it is due to either (i) a different conformation of the ICT state or (ii) another excited state species observable within the longer, ∼10 ns pulse duration. Its origin is the subject of further investigation by our group. All other bands can be attributed with confidence to the electronically decoupled ICT state [12] and the discussion will focus on these. It will be seen that our interpretations of the ICT state spectra of d_4 (Fig. 2a and b) are in full agreement with results obtained from the spectra of d_0 (Fig. 2c and d), d_6 and ^{15}N [12].

According to the characteristic frequency shifts on going from d_0 to d_4 (Section 3.1), the strong features of d_4 at 1553, 726 and 847 cm^{-1} are recognised as counterparts of the d_0 bands at 1597 ($\Delta\nu = 26\,cm^{-1}$), 756 ($\Delta\nu = 30\,cm^{-1}$) and 1170 ($\Delta\nu = 323\,cm^{-1}$) cm^{-1}. Their assignments to the ring 8a, 1 and 9a modes are thus straightforward.

It has been shown that the frequencies of modes related to the amino vibrations of the ICT states of d_0 and d_6 resemble those of protonated DMA, DMA-H^+ and DMA-d_6-H^+, respectively [12]. This analogy is also expected between d_4 and d_5-H^+ and it can be seen from Table 1 that the 726 and 847 cm^{-1} band of d_4 have corresponding bands for d_5-H^+ at 725 and 873 cm^{-1}, respectively. The bands observed for d_5-H^+ are, therefore, useful in identifying other bands of the ICT state of d_4. Thus, the 1271 cm^{-1} band observed in d_4 has been attributed to a mode dominated by the ν(ph-N) vibration, corresponding to the 1283 cm^{-1} band of d_5-H^+ (Table 1). Its counterpart in d_0 is the 1281 cm^{-1} band, as determined by spectra taken of DMABN with ^{15}N-amino isotopic labelling [12].

As for the ground state, the mode dominated by the ν(ph-CN) motion (1221 cm^{-1} band) of the ICT state of d_0 (Fig. 2c and d) disappears in the d_4 spectra (Fig. 2a and b). It is certain that one of the two bands at ∼1100, 1083 or 1105 cm^{-1}, corresponds to the ground state band of d_4 at 1114 cm^{-1} (the 7a mode, Table 1), however, it is not certain which of them relates to the 7a mode. With one of them attributed to this mode, the other might be assigned to one of the symmetric amino methyl rocking modes (ρ'_{me}) whose frequency is recorded at 1093 cm^{-1} in d_5-H^+. The counterpart of the ρ'_{me} mode in the ground state of d_4 is at 1096 cm^{-1} (Table 1).

The 1160 cm^{-1} band of d_4 (Fig. 2a) was assigned to another methyl rocking mode (ρ_{me}) corresponding to the ground state band at 1166 cm^{-1} (Fig. 1a). Our DFT calculations show that this mode is due to an almost pure methyl group vibration [26]. The very small change in frequency

Table 1
Frequencies (cm^{-1}) and assignments of resonance Raman bands observed for the ground, ICT and lowest triplet state of DMABN-d_4[a]

DMABN-d_4				DMA-d_5		
Tentative assignment	Ground state	ICT state	Triplet state	d_5[b]	d_5-H^+[c]	d_5^+[b]
C≡N	2218 (1.00)	2095 (1.00)	2028 (1.00)			
CC (8a)	1577 (0.62)	1553 (1.03)	1541 (1.13)	1575		1528
CC (8b)	1523 (0.22)			1542		
CC (19a) + ν(ph-N)	1417[d]		1259 (0.23)	1400	1370	1268
Methyl deformation	1504 (0.72)	1474 (0.01)	1480 (0.98)	1485		1475
Methyl deformation	1463 (0.31)	1447 (0.03)	1441 (0.38)	1455		
CC (19b)	1372 (0.10)	1308 (0.12)[e]		1361[f]		
ν(ph-N) (13)	1327 (0.15)	1271 (0.22)	1396 (1.10)	1298	1283	1387
ν(ph-N) + ν(ph-CN)	1114 (0.21)	1105 (0.07)	1102 (0.38)			
Ring CH in plane bending (9a)	875 (0.53)	847 (0.30)	815 (0.12)	874	873	875
Methyl rocking mode (ρ_{me})	1166 (0.10)	1160 (0.45)	1166 (0.12)	1140		1140
Methyl rocking mode (ρ'_{me})	1096[d]	1083 (0.27)	1079 (0.08)		1093	
$\nu^s(NC_2)$	944 (0.19)	899 (0.01)[e]	928 (0.10)	945	898	
Ring breathing (1)	763 (0.57)	726 (0.71)	708 (0.05)[e]	707	725	

[a] Relative intensities are indicated in parentheses. Data of DMA-d_5, its radical cation and hydrogen protonated counterpart are included for comparison.
[b] See [32].
[c] See [34].
[d] Not observed here due to no resonance enhancement at the 330 nm excitation wavelength.
[e] Weak feature whose assignment is uncertain.
[f] See [33].

of this mode on going from the ground to ICT or triplet (Table 1) state implies that the methyl group is barely affected by photo-excitation. It should be pointed out that this information can be obtained only from the d_4 spectra, because the corresponding bands for d_0, d_6, and ^{15}N, as indicated by the DFT computation, are due to modes having a substantial additional contributions from the ring motions [26,36]. The frequency of this band in d_0 shifts down by $\sim$54 cm^{-1} on going from the ground (1167 cm^{-1} [12,26]) to the ICT state (1116 cm^{-1}, Fig. 2c). The downshift is probably due to the frequency decrease in the ring vibrations rather than a change in conformation of the methyl group.

Several weak bands, 1474, 1447, 1308 and 899 cm^{-1}, of d_4 (Fig. 2a) were assigned as listed in Table 1. Their attribution is quite tentative due to the low intensities of these bands.

From Table 1, it can be seen that the frequency shifts for the corresponding bands on going from the ground to ICT state show the same trends and extent in d_4 as d_0 [12]. This is exemplified by C≡N ($\Delta\nu \approx 120\,cm^{-1}$), the ring modes 8a and 1 ($\Delta\nu \approx 20-30\,cm^{-1}$), and especially by the mode dominated by ν(ph-N) ($\Delta\nu \approx 56\,cm^{-1}$ in d_4, $\sim$96 cm^{-1} in d_0 [12]). This is in agreement with the molecular orbitals and frequencies of the ICT state suggested by theoretical calculations [4,43–45]. According to Dreyer and Kummrow [4], the frequency downshift of the ν(ph-N) dominated mode from the ground to the ICT state is essential evidence supporting the TICT model and rules out the PICT model. The close analogy of the C≡N and ring local mode frequencies of the ICT state to those found in the benzonitrile radical anion [46] indicates full charge transfer from the amino to benzonitrile group, and thus gives further support for the electronic decoupling envisaged by the TICT model. In the TRIR study performed by Hashimoto and Hamaguchi [13], observation of a large infrared intensity in the C≡N band suggests the transferred electron is delocalised over the whole benzonitrile moiety. In addition, a strong resemblance has also been found for the amino related mode frequencies of the ICT state of d_0/d_4 and protonated DMA, DMA-H^+/d_5-H^+. It has been shown that, in contrast to the mainly sp^2 (conjugated) conformation in neutral DMA, the amino group adopts the pyramidal sp^3 hybridisation conformation (electronically decoupled) in DMA-H^+ [34,47]. The resemblance strengthens the view of electron decoupling of the amino group from the ring π system in the ICT state and the results also imply some pyramidal character of the ICT state amino conformation. Theoretical studies [43,44,48] show that a wagging motion of the DMABN amino group alone cannot lead to a stable highly polar excited state (17 D [8]). Thus, according to our results, a mainly twisted structure combined with some wagging of the amino group seems to be the most realistic conformation for the ICT state. Such a structure has been suggested by a CASSCF study of DMABN by Serrano-Andres et al. [6].

3.3. The triplet state

The 2028 cm^{-1} C≡N frequency recorded here coincides with the triplet TRIR frequency recorded by Hashimoto and Hamaguchi [13]. Bands of d_4 at 1541 (1564 cm^{-1} in d_0, $\Delta\nu = 23\,cm^{-1}$) and 815 cm^{-1} (1170 cm^{-1} in d_0, $\Delta\nu = 355\,cm^{-1}$) (Fig. 3) are certainly due to the ring modes 8a and 9a, respectively. Being insensitive to ring deuteration, d_4

bands at 1480, 1441, 1166, 928 cm^{-1} (Fig. 3a) are vibrations related to the methyl or amino groups (two methyl deformation modes, methyl rocking (ρ_{me}) and $\nu^s(NC_2)$ mode, respectively). The 1102 cm^{-1} band was assigned to the unique d_4 mode 7a corresponding to the 1114 cm^{-1} band of the ground state (Fig. 1a) [26].

The weak feature observed in d_0 at 1086 cm^{-1} (Fig. 3b) with a corresponding band at 1079 cm^{-1} in the d_4 spectrum (seen as a shoulder in Fig. 3a), not identified before, can now be attributed to the methyl rocking mode (ρ'_{me}) due to its insensitivity to ring deuteration. The mode is observed at 1107 and 1096 cm^{-1} (Table 1) in the ground state of d_0 and d_4, respectively [26].

The strongest band at 1396 cm^{-1} and the middle intensity one at 1259 cm^{-1} (Fig. 3a) remain difficult to identify. Assignment to 19a and ν(ph-N) respectively is rejected for the following reasons. From our previous time-resolved resonance Raman study on d_0, d_6 and ^{15}N and a comparison of the ν(ph-N) frequency for ground (1377 cm^{-1}) and triplet (1361 cm^{-1}) states in d_0, a similar amino conformation, i.e. planar or near planar geometry, has been suggested for the triplet state [25]. However, in the case of d_4, with the ground state ν(ph-N) frequency observed at 1327 cm^{-1} (Fig. 1a, Table 1), it is unreasonable to associate this with the 1259 cm^{-1} band (Fig. 3a) seen in the triplet state spectrum. The ~68 cm^{-1} downshift is far greater than expected.

The ~190 cm^{-1} down shift of the C≡N stretch on going from ground (2218 cm^{-1}, Fig. 1a) to triplet (2028 cm^{-1}, Fig. 3a) state indicates a significant decrease of the C≡N triplet bond order. This reflects the way the negative charge is localised on the cyano group anti-bonding orbital in the triplet state of d_4. It has been shown that the ring, remaining conjugation with the amino group, acts as the donor of the negative charge in the triplet state when compared with the ground state [25]. We notice that resonance Raman studies of the radical cation of DMA, DMA^+, performed by Brouwer and Wilbrandt [32] and Poizat et al. [33] suggest that DMA^+ possesses an analogous conjugated structure. Indeed, the similarity between the dimethylaniline subgroup of the triplet state of d_0 to DMA^+ is reflected by the comparable frequencies. For example, the 1564 (8a), 1441 (19a), 1361 (ν(ph-N)), 1170 (9a), 1150 (ρ_{me}) cm^{-1} bands of the triplet state of d_0 (Fig. 3b) having their corresponding bands in DMA^+ at 1568, 1478, 1366, 1203 and 1163 cm^{-1} [32,33]. Parallel observations can be made for d_4 and $d_5{}^+$, the 1541 (8a), 1480 (δ_{me}), 815 (9a), 1166 (ρ_{me}) cm^{-1} bands observed in the triplet state of d_4 having corresponding bands in $d_5{}^+$ at 1528, 1475, 875, 1140 cm^{-1} (Table 1). The experimental and theoretical resonance Raman study of DMA^+ and its various isotopomers performed by Brouwer and Wilbrandt [32] show that ring deuteration causes a shift of the 19a mode from a frequency above that of ν(ph-N) to one below it. The two modes were found at 1268 (19a) and 1387 (ν(ph-N)) cm^{-1} in $d_5{}^+$ (Table 1), respectively. From this, we attribute the 1259 and 1396 cm^{-1} bands of d_4 (Fig. 3a) to the 19a and ν(ph-N) modes, respectively.

It has been shown that the response of the ν(ph-N) and 19a modes to ring deuteration is very different in neutral DMA and the radical cation of DMA. As mentioned above, DMA and DMA^+ have analogous properties to the ground and triplet states, respectively, of DMABN. On one hand, a near planar structure is determined for neutral DMA and ground state DMABN (Section 3.1), where frequency downshifts, $\Delta\nu = 50$ and 100 cm^{-1} for ν(ph-N) and 19a modes, respectively, are found for both compounds on going from normal to the ring deuterated isotopomers. Compared to the typical downshift (~20–30 cm^{-1}) for the other ring CC stretching modes (such as 8a and 1, see above), the much greater decrease in frequency for these two modes is due to changes in vibrational coupling associated with these modes in the ring deuterated compound (Section 3.1). On other hand, a planar quinoidal structure has been suggested and confirmed by theoretical calculation for DMA^+ and it was established that the unusual isotopic effect mentioned in the preceding paragraph can be considered as a typical feature of such a conformation [49,50]. We, therefore, propose the same structure for the triplet state of d_0/d_4. The large downshift observed for the 19a mode on going from the ground (1527/1417 cm^{-1} for d_0/d_4) to triplet (1442/1259 cm^{-1} for d_0/d_4) state supports this quinoidal conformation since it requires a substantial lengthening of the C_1–C_2 bond whose stretching is mainly responsible for the 19a mode [35].

It is worthwhile to point out that discrimination of planar from near planar geometry for the triplet state amino conformation results from our analysis of the d_4 spectra presented here and was not achieved in our previous work [25]. The very close resemblance in frequencies of modes related to both the ring and amino groups in the triplet state of d_0/d_4 to $DMA^+/d_5{}^+$ indicates a complete charge separation character for the triplet state with the separated charge localisatised on the cyano group. This is in accordance with the 1,4-biradical character suggested by Carsey et al. [51] for the triplet state of typical para-disubstituted benzene of type D-ph-A. The geometric and electronic character of the triplet state proposed here is also in good agreement with published results obtained by various experimental methods, such as phosphorescence [18,19], transient absorption [19,20], dipole moment (12 D [8]) and ESR [19,52] measurements. It is also consistent with the theoretical results [5,6,22,23].

The 532 nm probe wavelength used in the ns-TR^3 experiments falls into the second transition [19,20] (peaking at ~550 nm) of the triplet state of DMABN. We notice that in the 650-1600 cm^{-1} spectral region, besides the frequencies and isotopic shift behaviour, intensity patterns of the triplet spectra of d_0/d_4 parallel those of $DMA^+/d_5{}^+$ obtained using 467 nm Raman excitation [32,33] (absorption maximum is ~475 nm [53]). This implies that the resonance absorption of the triplet state of d_0/d_4 at 532 nm and $DMA^+/d_5{}^+$ at 467 nm are of a similar nature, i.e. leading to comparable structural distortions and variations in the molecular orbitals associated with the resonant chromophore. The red shift of

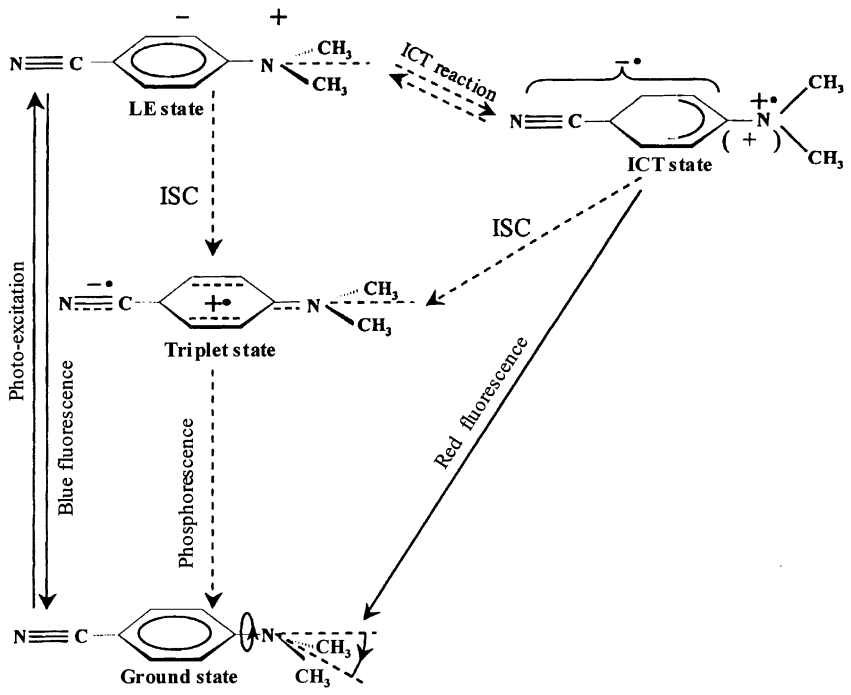

Scheme 1. Proposed structures of the ground, LE, ICT and triplet states of DMABN [3,4,11–13,16,19,25,37]. The radiative and non-radiative processes are indicated by solid and dotted, respectively, lines with arrows.

the absorption band from $DMA^+/d_5{}^+$ to d_0/d_4 is probably due to an additional conjugation effect caused by the cyano group in d_0/d_4.

4. Summary

The transient Raman spectra of the ICT and triplet states of d_4 can be explained in terms of the same electronic and geometric properties inferred from corresponding spectra of d_0, d_6 and ^{15}N [12,25]. This confirms our previous conclusions regarding the structures of the ICT and triplet state of DMABN. However, the unique isotopic effect observed in the Raman spectra of d_4 provides unequivocal evidence to clarify the planar structure and the localisation of a complete charge separation onto the cyano group in the triplet state.

Scheme 1 shows properties of the ground, LE, ICT and triplet states of DMABN. The ground state is according to the structure established by X-ray diffraction [37]. From both experimental [2,3,38] and theoretical [4–6,44] work, the LE state has been suggested to be planar, with a small extent of ICT as indicated by a slight increase in dipole moment [8] (10 D) compared to the ground state (6.7 D). It is also supported by a small frequency down shift ($\Delta\nu \approx 40\,cm^{-1}$) of the C≡N mode on going from the ground to the LE state [2]. The ICT and triplet states are as described above and in our previous work [12,25]. Combining the temporal evolution of transient absorption [2,19,25,40] and the results of time-resolved fluorescence studies [8,54–56] reported before, the photo-induced ICT reaction, the non-radiative deactivation channels of the singlet excited states and the phosphorescence process from the triplet state are also indicated in the scheme.

Acknowledgements

We are grateful to the EPSRC for financial support through Grants GR/K20989 and GR/L84001. We thank Dr. Ian Clark for his assistance in the ns-TR^3 experiments. This work was carried out within the Central Laser Facility, CLRC Rutherford Appleton Laboratory.

References

[1] E. Lippert, W. Rettig, V. Bonacic-Koutecky, F. Heisel, J.A. Miehe, Adv. Chem. Phys. 68 (1987) 1.
[2] W.M. Kwok, C. Ma, D. Phillips, P. Matousek, A.W. Parker, M. Towrie, J. Phys. Chem. A 104 (2000) 4189.
[3] C. Chudoba, A. Kummrow, J. Dreyer, J. Stenger, E.T.J. Nibbering, T. Elsaesser, K.A. Zachariasse, Chem. Phys. Lett. 309 (1999) 357.
[4] J. Dreyer, A. Kummrow, J. Am. Chem. Soc. 122 (2000) 2577.
[5] A.B.J. Parusel, G. Köhler, M. Nooijen, J. Phys. Chem. A. 103 (1999) 4056.
[6] L. Serrano-Andres, M. Merchan, B.O. Roos, R. Lindh, J. Am. Chem. Soc. 117 (1995) 3189.
[7] K. Rotkiewicz, K.H. Grellmann, Z.R. Grabowski, Chem. Phys. Lett. 19 (1973) 315.
[8] W. Schuddeboom, S.A. Jonker, J.M. Warman, U. Leinhos, W. Kuhnle, K.A. Zachariasse, J. Phys. Chem. 96 (1992) 10809.

[9] K.A. Zachariasse, M. Grobys, T. Von der Haar, A. Hebecker, Y.V. Ilchev, Y.-B. Jiang, O. Morawski, W. Kuhnle, J. Photochem. Photobiol. A: Chem. 102 (1996) 59.
[10] A.L. Sobolewski, W. Sudholt, W. Domcke, Chem. Phys. Lett. 259 (1996) 119.
[11] W.M. Kwok, C. Ma, P. Matousek, A.W. Parker, D. Phillips, W.T. Toner, M. Towrie, Chem. Phys. Lett. 322 (2000) 395.
[12] W.M. Kwok, C. Ma, P. Matousek, A.W. Parker, D. Phillips, W.T. Toner, M. Towrie, S. Umapathy, J. Phys. Chem. A. 105 (2001) 984.
[13] M. Hashimoto, H. Hamaguchi, J. Phys. Chem. 99 (1995) 7875.
[14] H. Okamoto, J. Phys. Chem. A 104 (2000) 4182.
[15] B. Mennucci, A. Toniolo, J. Tomasi, J. Am. Chem. Soc. 122 (2000) 10621.
[16] T. Okada, M. Uesugi, G. Kohler, K. Rechthaler, K. Rotkiewicz, W. Rettig, G. Grabner, Chem. Phys. 241 (1999) 327.
[17] N. Chattopadhyay, J. Rommens, M. Van der Auweraer, F.C.D. Schryver, Chem. Phys. Lett. 264 (1997) 265.
[18] R. Günther, D. Oelkrug, W. Rettig, J. Phys. Chem. 97 (1993) 8512.
[19] G. Köhler, G. Grabner, K. Rotkiewicz, Chem. Phys. 173 (1993) 275.
[20] Y. Wang, J. Chem. Soc., Faraday Trans. 84 (1988) 1809.
[21] N. Chattopadhyay, M. Van der Auweraer, F.C.De. Schryver, Chem. Phys. Lett. 279 (1997) 303.
[22] P. Purkayastha, P.K. Bhattacharyya, S.C. Bera, N. Chattopadhyay, Phys. Chem. Chem. Phys. 1 (1999) 3253.
[23] C. Bulliard, M. Allan, G. Wirtz, E. Haselbach, K.A. Zachariasse, N. Detzer, S. Grimme, J. Phys. Chem. A 103 (1999) 7766.
[24] J. Lipinski, H. Chojnacki, Z.R. Grabowski, K. Rotkiewicz, Chem. Phys. Lett. 70 (1980) 449.
[25] C. Ma, W.M. Kwok, P. Matousek, A.W. Parker, D. Phillips, W.T. Toner, M. Towrie, J. Phys. Chem. A 105 (2001) 4648.
[26] W.M. Kwok, I. Gould, C. Ma, M. Puranik, S. Umapathy, P. Matousek, A.W. Parker, D. Phillips, W.T. Toner, M. Towrie, Phys. Chem. Chem. Phys. 3 (2001) 2424.
[27] P. Matousek, A.W. Parker, P.F. Taday, W.T. Toner, M. Towrie, Opt. Commun. 127 (1996) 307.
[28] M. Towrie, A.W. Parker, W. Shaikh, P. Matousek, Meas. Sci. Technol. 9 (1998) 816.
[29] P. Matousek, M. Towrie, A. Stanley, A.W. Parker, Appl. Spectrosc. 53 (1999) 1485.
[30] R.H. Mitchell, Y. Chen, J. Zhang, Org. Prep. Proced. Int. 29 (1997) 715.
[31] L. Friedman, H. Shechter, J. Org. Chem. 26 (1961) 2522.
[32] A.M. Brouwer, R. Wilbrandt, J. Phys. Chem. 100 (1996) 9678.
[33] O. Poizat, V. Guichard, G. Buntinx, J. Chem. Phys. 90 (1989) 4697.
[34] V. Guichard, A. Bourkba, M-F. Lautie, O. Poizat, Spectrochim. Acta 45A (1989) 187.
[35] G. Varsanyi, in: L. Lang (Eds.), Assignments for Vibrational Spectra of 700 Benzene Derivatives, Vol. I, Adam Hilger, London, 1974.
[36] H. Okamoto, H. Inishi, Y. Nakamura, S. Kohtani, R. Nakagaki, Chem. Phys. 260 (2000) 193.
[37] A. Heine, R.H. Irmer, D. Stalke, W. Kuhnle, K.A. Zachariasse, Acta Cryst. B50 (1994) 363.
[38] O. Kajimoto, H. Yokoyama, Y. Ooshima, Y. Endo, Chem. Phys. Lett. 179 (1991) 455.
[39] R. Cervellati, A.D. Borgo, D.G. Lister, J. Mol. Struct. 78 (1982) 161.
[40] T. Okada, M. Uesugi, G. Kohler, K. Rechthaler, K. Rotkiewicz, W. Rettig, G. Grabner, Chem. Phys. 241 (1999) 327.
[41] M. Forster, R.E. Hester, J. Chem. Soc., Faraday Trans. II 77 (1981) 1535.
[42] C. Ma, W.M. Kwok, P. Matousek, A.W. Parker, D. Phillips, W.T. Toner, M. Towrie, J. Raman Spectrosc. 32 (2001) 115.
[43] A.B.J. Parusel, G. Kohler, S. Grimme, J. Phys. Chem. A 102 (1998) 6297.
[44] A-D. Gorse, M. Pesquer, J. Phys. Chem. 99 (1995) 4039.
[45] G. Calzaferri, R. Rytz, J. Phys. Chem. 99 (1995) 12141.
[46] I. Juchnovski, C. Tsvetanov, I. Panayotov, Monatsh. Chem. 100 (1969) 1980.
[47] R. Chandrasekaran, Acta Cryst. B25 (1969) 369.
[48] W. Sudholt, A.L. Sobolewski, W. Domcke, Chem. Phys. 240 (1999) 9.
[49] G. Buntinx, A. Benbouazza, O. Poizat, V. Guichard, Chem. Phys. Lett. 153 (1988) 279.
[50] S. Yamaguchi, N. Yoshimiza, S. Maeda, J. Phys. Chem. 82 (1978) 1078.
[51] T.P. Carsey, G.L. Findley, S.P. McGlynn, J. Am. Chem. Soc. 101 (1979) 4502.
[52] P.J. Wagner, M.L. May, J. Phys. Chem. 95 (1991) 10317.
[53] Shida T. Electronic Absorption Spectra of Radical Ions, Vol. 34, Elsevier, Amsterdam, 1988, p. 208.
[54] P. Changenet, P. Plaza, M.M. Martin, Y.H. Meyer, J. Phys. Chem. A 101 (1997) 8186.
[55] J.D. Simon, S.G. Su, J. Phys. Chem. 94 (1990) 3656.
[56] E.M. Gibson, A.C. Jones, D. Phillips, Chem. Phys. Lett. 136 (1987) 454.